Structure Damage Detection Using Neural Network with Multi-Stage Substructuring

Article *in* Advances in Structural Engineering · February 2010

DOI: 10.1260/1369-4332.13.1.95

CITATIONS
27

READS
616

3 authors:

Norhisham Bakhary
Universiti Teknologi Malaysia
25 PUBLICATIONS **172** CITATIONS
SEE PROFILE

Hong Hao
Curtin University
551 PUBLICATIONS **7,744** CITATIONS
SEE PROFILE

Andrew John Deeks
University College Dublin
111 PUBLICATIONS **2,042** CITATIONS
SEE PROFILE

Structure Damage Detection Using Neural Network with Multi-Stage Substructuring

Norhisham Bakhary[1,*], Hong Hao[2] and Andrew J. Deeks[2]

[1]Faculty of Civil Engineering, Universiti Teknologi Malaysia, Skudai, Johor, Malaysia
[2]School of Civil and Resource Engineering, The University of Western Australia, Australia

(Received: 28 August 2008; Received revised form: 14 April 2009; Accepted: 22 April 2009)

Abstract: Artificial neural network (ANN) method has been proven feasible by many researchers in detecting damage based on vibration parameters. However, the main drawback of ANN method is the requirement of enormous computational effort especially when complex structures with large degrees of freedom are involved. Consequently, almost all the previous works described in the literature limited the structural members to a small number of large elements in the ANN model which resulted ANN model being insensitive to local damage. This study presents an approach to detect small structural damage using ANN method with progressive substructure zooming. It uses the substructure technique together with a multi-stage ANN models to detect the location and extent of the damage. Modal parameters such as frequencies and mode shapes are used as input to ANN. To demonstrate the effectiveness of this approach, a two-span continuous concrete slab structure and a three-storey portal frame are used as examples. Different damage scenarios have been introduced by reducing the local stiffness of the selected elements at different locations in the structures. The results show that this technique successfully detects all the simulated damages in the structure.

Key words: damage detection, neural networks, substructure, modal data.

1. INTRODUCTION

Damage assessment using vibration based data has been receiving significant attention for the last three decades. Since the early work by Cawley and Adam (1979), dynamic parameters such as natural frequencies and mode shapes have been widely used for damage detection. Various methods have been researched and developed to derive an effective and accurate procedure to locate damage and estimate the damage severity in structures using those parameters.

Damage detection from modal data is an inverse process that relies on the relationship between the modal parameters and the structural properties. If there are changes in properties of the structure, the modal parameters will change accordingly. Using the modal parameters and analysing their changes, the damage locations and damage severities can be determined. This rigorous relationship allows the application of mathematical algorithms in order to perform the inverse analysis. Most current approaches use conventional rule-based mathematical algorithms such as optimization and fuzzy logic. However, those conventional rule-based methods are very time consuming and may require some arbitrary decisions by the user.

The rapid development of computer technologies has increased the possibility of using these methods for

*Corresponding author. Email address: bakhary@utm.my; Fax: +60-7-5566-157; Tel: +60-7-5532-517.
Associate Editor. Y. Xia.

practical damage detection. The artificial neural network (ANN) method is one technique that has been intensively studied. ANN is a mathematical model of theoretical mind and brain activity. Its ability in pattern recognition and error tolerance makes ANN useful in establishing a nonlinear relationship between its inputs and outputs. Another advantage of ANN over rule-based system is that ANN has the interpolation capability to produce appropriate results for noisy inputs. The basic idea of using ANN for damage detection is to build a model to provide a relationship between modal parameters and structural parameters through a training process. Once the relationship is established, the trained ANN model is then capable of detecting damage from modal data. The success of ANN applications in damage detection using vibration parameters in civil structures was first reported by Wu *et al.* (1992) and, since then, has drawn considerable attention. Many successful applications of ANN to damage detection in numerical and laboratory structure models have been reported (Barai *et al.* 1995; Worden *et al.* 1997; Chang *et al.* 2000; Chen *et al.* 2002; Zapico *et al.* 2003; Bakhary *et al.* 2007). Most of them have been limited to example structures with a small number of degrees of freedom and with quite significant damage levels. For example Zhao *et al.* (1998) used ANN to identify damage of a nine meter beam with 18 elements. The damage was introduced as a stiffness reduction of 15% to 45% of the original stiffness value of each element. Chang *et al.* (2000) employed ANN to detect damage in an eight-element RC beam. The damage considered was stiffness reduction of 10% to 25% of design stiffness values in each element. Pandey and Barai (1995) applied ANN to detect damage in a 0.5 meter long 21-bar truss bridge model. The damage scenarios considered were formed by reducing the cross sectional area of a small number of truss members

Examples of successful identification of local small damage in structures by ANN are quite limited. This is because a fine finite element mesh is needed to detect small local damage in a structure. This results in a large number of elements in the finite element model of a structure, and hence a high dimension network in the ANN model. It then requires significant computational time and computer memory to train the ANN model. The computational time and computer memory needed to train an ANN model increases dramatically with increasing number of structural degrees of freedom. Therefore, in most examples, rather large elements are used in structure model to reduce the degrees of freedom. Since a large element is insensitive to a small damage, severe damage scenarios are usually assumed to successfully apply the ANN model to damage identification.

Several attempts have also been made to apply ANN to complex structures with large degrees of freedom. In those studies, the structures are divided to a small number of segments. Each segment consists of several elements (Ni *et al.* 1998; Lee *et al.* 2002; Xu *et al.* 2006) and all the elements within the same segment are assumed to have the same material properties. This simplification reduces the number of variables and makes training ANN model efficient. However, it also makes the ANN model insensitive to small local damage, and therefore reduces its ability to provide reliable structure damage detection.

To overcome the difficulties discussed above, Yun and Bahng (2000) developed a technique to identify damage in probable damage areas using a substructure technique. However, early and sometimes subjective judgement using conventional techniques such as visual inspection is required to select the probable damage areas. To improve this method Ko *et al.* (2002) have developed a three-stage identification technique. In their study, a novel technique utilizing auto associative neural network is used in the first stage to identify the damage existence in the structure, followed by a combination of modal curvature index and modal flexibility index to identify the damage area in the second stage. Once a probable damage area is identified, an ANN model is used to determine the damage location and severity in the third stage. The disadvantages of this method are: (i) the novel detection approach used in the first stage may not be sensitive enough to trigger the alarm for damage existence, as shown in two of the twelve cases analysed in the study; (ii) modal curvature index and modal flexibility index are sometimes unable to provide accurate identification, especially when damage is near the support area, as demonstrated in the study; (iii) if the damage occurs in multiple areas, expensive computation is still required in the third stage to train the ANN model as the number of areas that contain damages increases.

From the studies above, it is obvious that a single stage ANN is not feasible to detect damage in structures with many degrees of freedom, therefore a multi-stage ANN method is proposed in this study. The feasibility of multi-stage ANN in damage detection also has been demonstrated by Pillai and Shankar (2008) using counterpropagation ANN in the first stage and backpropagation in the second stage. Different from the above study, this paper presents an approach to detect small structural damage using ANN with a progressive substructuring technique. A multi-stage ANN model is proposed as a basic structure for the damage detection system. This approach uses a minimum number of substructures at each stage and uses only the data from the first few modes to identify

structure damage. Because the damages are identified progressively, the accuracy of the damage identification is not compromised while the computational time and the required computer memory are kept relatively small by this approach. A two-span concrete slab and a one-span three-storey frame with various damage scenarios in single and multiple locations are numerically simulated and used as the examples in this study. The effectiveness of the proposed method is then compared with the conventional one-stage ANN method. A sensitivity study is also performed to obtain the relationship between damage detectability and the substructure size.

2. METHODOLOGY

2.1. Substructure Technique

Several studies have applied the substructure technique for structural condition identification. Oreta *et al.* (1994) and Koh *et al.* (2003) demonstrated the substructural approach derived from static condensation using a Genetic algorithm and Extended Kalman Filter to identify the physical properties in a specified damage area. As static condensation depends on the information from other part of the structure, the derivation of the substructure model is complicated and the computation is relatively time consuming. Moreover, certain prescribed rules are needed to apply those mathematical models. Recently, Yuen and Katafygiotis (2006) presented a probabilistic substructure identification and health determination method for linear systems using time history data. The authors proved that the condition of the substructure can be determined by considering acceleration only from the substructure of interest within a large structure.

In this study, the substructure is defined as an independent structure by assuming the fixed interface. The method was introduced by Hurty (1964), and is known as component mode synthesis (CMS). In CMS, the mode shape components are assembled to construct Ritz vectors, which are subsequently used to construct the mode shapes for the whole structure. This idea is adopted in the present study because any change of conditions in full structure will change the condition of some or all the substructures. Since frequency alone is not sufficient to detect damage location, the mode shape values of the full structure at points corresponding to the substructure are also used as the input variable. In each substructure, although the available mode shape points are limited, the components of the mode vectors of the substructure include most information regarding the stiffness parameters of the substructure.

In the present study, this substructure technique is applied together with a multi-stage ANN to identify local damage. This is done by dividing the full structure to several substructures. By doing this, each substructure can be represented by one ANN model, and thus each ANN model can be trained separately. This substantially reduces the number of unknowns in one ANN model, and hence improves the training quality and reduces the training time.

2.2. Artificial Neural Network

Without losing generality, the multi-stage ANN system used in this study is briefly discussed below. Figure 1 depicts the basic structure of the system.

The ANN model in the first stage is referred to as the *primary ANN* and the second stage is referred to as the *secondary ANN*. The primary ANN is used to identify the substructures that have suffered damage while the secondary ANN identifies the damage location and estimate the damage severities. Each primary ANN is trained to relate the frequencies and modes shapes of the full structure and frequencies of every substructure. The frequencies and mode shapes of the full structure are used as the inputs to the ANN model, while the outputs are the frequencies of every substructure. Both input and output data are obtained through a series of finite element analysis. The whole structure is considered in the analysis of the full structure while each of the substructures is analysed independently by assuming the boundary condition as fixed interface as mentioned earlier Once the relationship is established, the ANN model can be used to estimate the frequencies of each substructure from modal parameters of the full structure. The substructures that suffer damage can be identified from their frequency changes. In this study, the frequency change index (FCI) is defined as

$$FCI^i = 1 - \left(\frac{F^{i\prime}}{F^i} \right)^2 \tag{1}$$

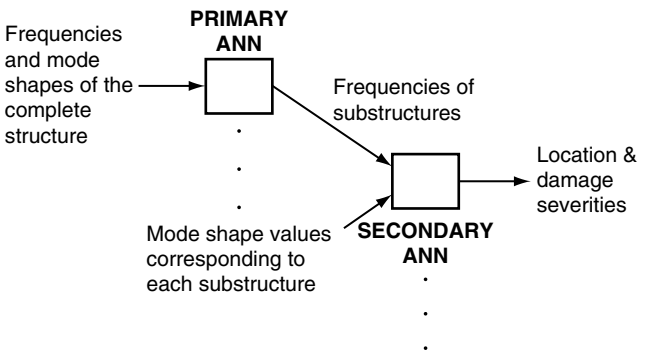

Figure 1. Structure of the two-stage ANN

$F^{i\prime}$ and F^{i} are calculated from the frequencies of the damaged and undamaged i^{th} substructure as:

$$F^{i} \text{ or } F^{i\prime} = \frac{\sum_{1}^{n} f^{n}}{n} \tag{2}$$

where f is the normalized predicted frequency of the i^{th} substructure and n is the mode number. The normalized frequencies are calculated by:

$$f^{n} = \frac{f_{p}^{n} - f_{\min}^{n}}{f_{\max}^{n} - f_{\min}^{n}} \tag{3}$$

where $f_p{}^n$ is the predicted nth modal frequency. $f_{max}{}^n$ and $f_{min}{}^n$ are the maximum and minimum frequencies used to train the model.

In the secondary ANN model, each substructure identified with frequency change by the primary ANN model is represented by a new independent ANN model to predict the E values (Young's modulus) of the elements in this substructure. The output of primary ANN model, together with the mode shape values of the full structure at nodal points corresponding to the substructure, are used as the input variables. The change of the stiffness parameter or the damage severity for each element is denoted by a stiffness reduction ratio (SRF), defined as:

$$SRF = 1 - \frac{E'}{E} \tag{4}$$

where E is the Young's modulus in the intact state and E' is that of the damaged state.

2.2.1. Design of primary ANN

As mentioned above, the primary ANN is designed to detect the existence of damage in any substructure based on the frequency changes of each substructure. For this purpose, the ANN in this stage is used to predict the frequencies of every substructure from the modal parameters of the full structure. If further resolution in the damaged location is needed, the substructure can be further divided to smaller sub-substructures, and this process can be repeated to any number of desired stages depending on the size of the substructure under consideration and the required accuracy of the identification results. For example, Figure 2 shows the two-stage primary ANN model.

In the figure, a two-stage primary ANN model is shown. In the first stage, the ANN (NN1S1) is used to predict the frequencies of two substructures. The outputs of the ANN in the first stage (frequencies) supplemented by mode shapes of the corresponding substructure obtained from the full structure analysis, are used as the inputs to the ANN in the second stage. For this example, the first substructure is further divided into another two substructures and NN2S2 is used to predict their frequencies and allow their conditions to be examined. In other words, if a damaged substructure is identified in the first stage, another ANN model corresponding to the damaged substructure can

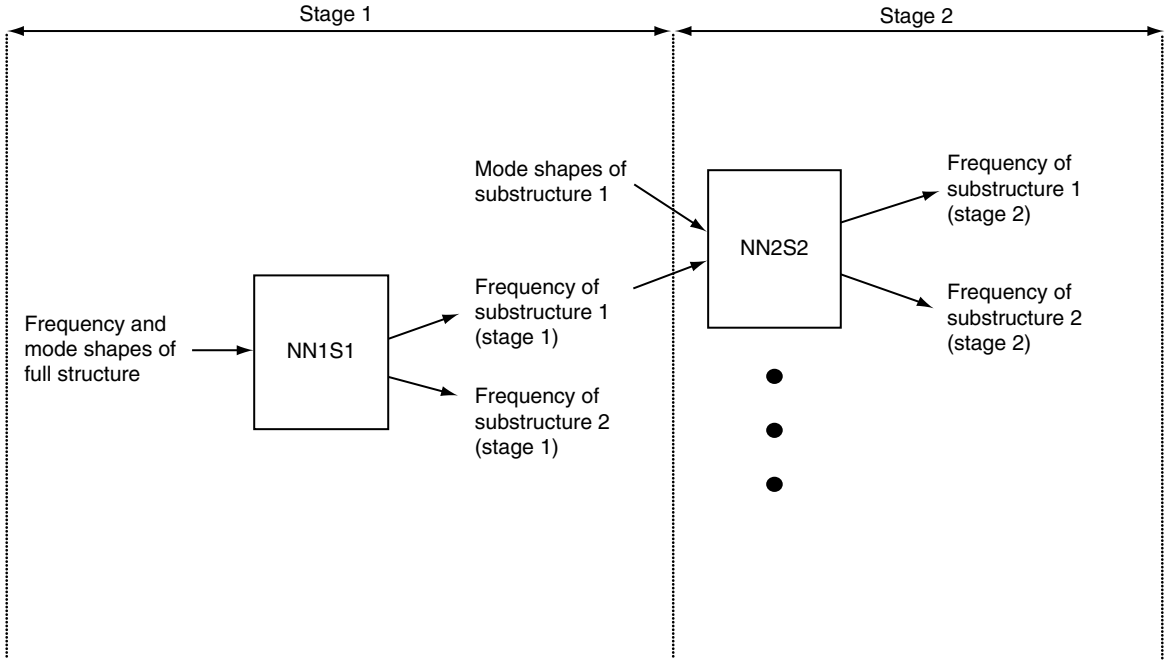

Figure 2. Schematic diagram of a two-stage primary ANN

be built in the second stage to increase the resolution of the damage location. At this stage, if needed, the measurement points can be refined by adding more measurement points focusing on the identified substructure. This process can be further extended to more stages. Since ANN models only need to be built for the damaged substructures, and the number of unknowns in each model can be kept to a minimum in the refinement process, this process will not substantially increase the computational time and the requirement of computer memory.

The ability of an ANN to recognize patterns is dependent on the similarity of given input data to the populations that are used to train the network. Hence, when the testing data is close to the training data, satisfactory output can be obtained.

For training, the damage cases are generated using finite element model. An orthogonal array is used together with Latin hypercube sampling method to reduce the number of simulations while maintaining the effect of every damage case (Chang *et al.* 2000). The vibration properties for the full structure and the substructures are computed using finite element analysis. The same material properties are used for the full structure and the corresponding substructures, and hence, any changes of condition in full structure will affect the condition of the corresponding substructure. For training the ANN models the frequencies and the mode shapes are used as the inputs. The training data for the ANN at the first stage are directly obtained from finite element model, while for the subsequent stages the frequencies are generated from the ANN model in the previous stage to reduce the effect of ANN prediction error propagation from the earlier stage. The generated frequencies are then combined with the mode shapes to form a set of input variables for the second stage ANN model. The same procedure applies if more than two stages are needed.

A multilayer neural network with one hidden layer is used to train the ANN models. Sigmoid functions are employed as non-linear activation functions for all layers. The ANN models are trained using the Levenberg Maquardt (trainlm) algorithm with an early stopping method to reduce the possibility of over-fitting. The performance of training is measured using mean square error (MSE):

$$MSE = \frac{1}{n}\sum_{j=1}^{n}(O_t - O_p)^2 \tag{5}$$

where O_t and O_p are the target and predicted outputs and n is the number of data.

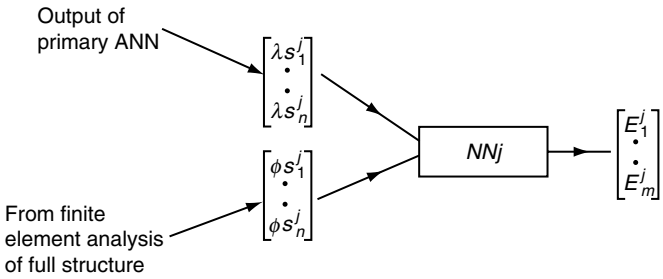

Figure 3. Schematic diagram of a secondary ANN

2.2.2. Design of secondary ANN

The secondary ANN receives information from the primary ANN and determines the location and severity of the damage. The frequencies of the substructures from primary ANN and the mode shapes of the corresponding substructure are used as the inputs to predict the E values of the segment in the identified substructure.

Figure 3 depicts the structure of the secondary ANN for substructure j. The input variables for ANN model (NNj) in the figure are modal frequencies ($\lambda_1^j ... \lambda_n^j$) and mode shapes ($\phi s_1^j ... \phi s_n^j$) of substructure j and the output variables are the E values of m elements in substructure j ($E_1^j ... E_m^j$). If more than one substructure is involved, each of them is represented by a different ANN model. Therefore, the ANN models can be designed independently.

The same training scheme used for the primary ANN is applied to this stage. Once trained, the ANN model is able to estimate the existence and severity of damage in each element in the respective substructure.

The change of the stiffness parameter or the damage severity for each element is denoted by a stiffness reduction ratio (SRF), defined as

$$SRF = 1 - \frac{E'}{E} \tag{6}$$

where E is the Young's modulus in the intact state and E' is that at the damage level of interest.

3. NUMERICAL EXAMPLE 1

A two-span concrete slab with dimensions of 6400 mm × 800 mm × 100 mm shown in Figure 4 is used as an example. The boundary conditions are idealized as pin supports at the middle span and at 200 mm from left and right end of the slab. The material properties are: $E = 3.2 \times 10^{10}\ N/mm^2$, $\rho = 2.45 \times 10^3\ kg/m^3$, $v = 0.2$. For damage detection purposes, the slab is divided to 32 segments as shown in Figure 5.

Four damage scenarios are simulated to assess the ANN performance as listed in Table 1. It is assumed that the mode shapes are measured at every 200 mm on the

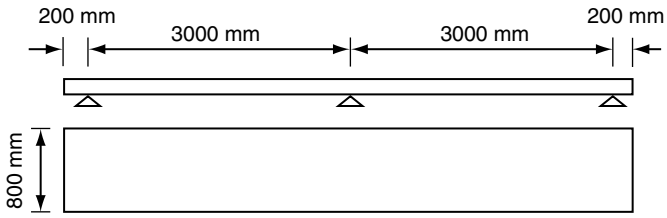

Figure 4. Dimension of the slab

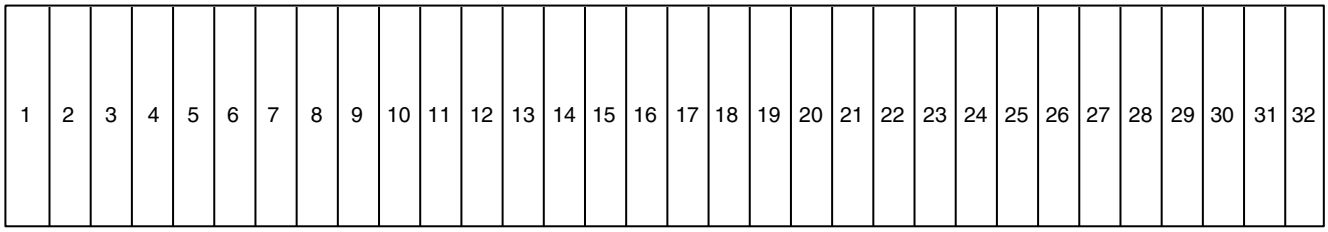

Figure 5. Segment of the slab

Table 1. Damage scenarios

Scenario	Element number	E value
1	7	0.95 × E
	8	0.95 × E
2	7	0.90 × E
	8	0.90 × E
3	5	0.85 × E
	6	0.85 × E
	7	0.85 × E
	8	0.85 × E
	9	0.85 × E
	10	0.85 × E
4	5	0.90 × E
	6	0.90 × E
	7	0.85 × E
	8	0.85 × E
	9	0.90 × E
	10	0.90 × E
	15	0.90 × E
	16	0.90 × E
	17	0.90 × E
	18	0.90 × E
	23	0.95 × E
	24	0.95 × E
	25	0.90 × E
	26	0.90 × E
	27	0.95 × E
	28	0.95 × E

centerline along the span length. Scenario 1 and 2 consist of damage at the middle of the first span (segment 7 & 8) with increasing damage severity. A severer damage case is simulated in scenario 3, where lower *E* values are applied to segments 5 to 10. In scenario 4, damage is assumed to occur in 16 segments in both spans and at the middle support. The modal analysis is conducted using finite element analysis, and the first three frequencies for these simulated damage scenarios are listed in Table 2.

In this example, the ANN is applied to detect the simulated damages. For the purpose of comparison the predictions of the conventional approach and the proposed technique are compared. The term 'conventional ANN' refers to the one-stage ANN technique where the output variables consist of the E values of all the elements.

3.1. Conventional ANN

First consider the one-stage ANN model for damage detection. The input variables for the ANN model are the first two modal frequencies and mode shapes of the slab and the outputs are *E* values of every segment. An ANN model with one hidden layer is applied. The number of hidden neuron is determined by trial and error. To train the ANN model, a data set containing 2000 damage instances is used. The data set is divided into two parts, 1600 instances for training and 400 for validation. In order to make sure that the training instances cover as many damage scenarios as possible, the combination of damage locations and severities is extracted using the orthogonal array (OA) method. The damage severities for each damage location are varied using Latin hypercube sampling. Since there are 32 segments on the slab and two levels of damage (damaged and undamaged), the combination of damage and undamaged cases over those segments is obtained by using OA 33.32.2.3 from a library of over 200 OAs maintained by Sloane (2007).

Table 2. First three frequencies of the undamaged and damaged structure

	Undamaged	Scenario 1	Scenario 2	Scenario 3	Scenario 4
Mode 1	18.540	18.481	18.417	18.028	17.928
Mode 2	28.873	28.788	28.698	28.255	27.623
Mode 3	73.646	73.554	73.454	72.472	72.157

Table 3. Performance of one-stage ANN model

Model	Training performance (MSE)	Validation performance (MSE)	Elapsed time (Second)
62-4-32	0.738	0.743	501.2
62-6-32	0.631	0.654	621.5
62-9-32	0.273	0.301	830.1
62-10-32	Out of memory	–	–
62-13-32	Out of memory	–	–

The ANN model is trained until one of the stopping criteria is met, i.e.

(i) The validation error increases for a specified number of iterations;
(ii) The training performance is less than the error goal of 0.001.

The training is conducted using a personal computer with Pentium 4 3.2 GHz processor and 2 GB memory and employing the Levenberg Maquardt (trainlm) algorithm with an early stopping method. Table 3 shows the training and validation performance of the one-stage ANN model with 4 to 13 hidden neurons. As indicated in the table, the training and validation performance improves when the number of hidden neurons increases, which means that higher numbers of hidden neurons are needed to successfully train this ANN model. However, increase the hidden neurons significantly increases the computational time and computer memory. When 10 or more neurons are introduced in hidden layer, it caused memory overflow of the computer system used in this study. This indicates that the current operating system memory is not sufficient to be used to train those ANN models. For a smaller number of hidden neurons (4, 6 and 9), the ANN models are trainable. However, the training performances are rather poor with relatively large MSE values. The training time also increases when the dimension of the ANN increases.

Figures 6(a) to 6(d) illustrates the comparison between actual and predicted E values when the simulated damage scenarios are applied to ANN model (62-9-32). For scenario 1 and 2, the damages at segment 7 and 8 are undetectable. For scenario 3, the damage locations are detected, however their severities are underestimated. There are also some false predictions. For scenario 4, damages at the left span and at the center support are correctly located but the severity is still poorly estimated. The damages at the right span are not detected. There are also some false predictions on the slab. These results show that the trained ANN model does not reliably predict the simulated damages in the concrete slab. This is because the ANN model is insufficiently trained and the relationship between inputs and outputs is not well established. If the model is trained with more hidden neurons, its reliability in predicting damages will be improved, but the computational time and required computer memory prevent using more than 10 hidden neurons. This example demonstrates that a one-stage ANN model cannot be efficiently applied to estimate a large number of parameters, because the large number of outputs will result in a large dimension of weights in the interconnected neurons, and that will lead to the requirement of more computational time and a large amount of computer memory. For this reason, many publications where damage detection is performed using an ANN model limit the number of parameters to be determined to a minimum, as discussed above.

3.2. ANN Damage Detection Using Substructure Technique

To apply the proposed approach, the slab is divided to 4 substructures. Each is 1.6m in length and consists of 8 segments as illustrated in Figure 7. Two-stage ANN models are applied in the primary level to assess the condition of substructures. Then a secondary level ANN model is applied to substructures with detected condition changes in the primary level in order to predict the location and severity of damage in the substructure. Figure 8 shows the ANN architecture.

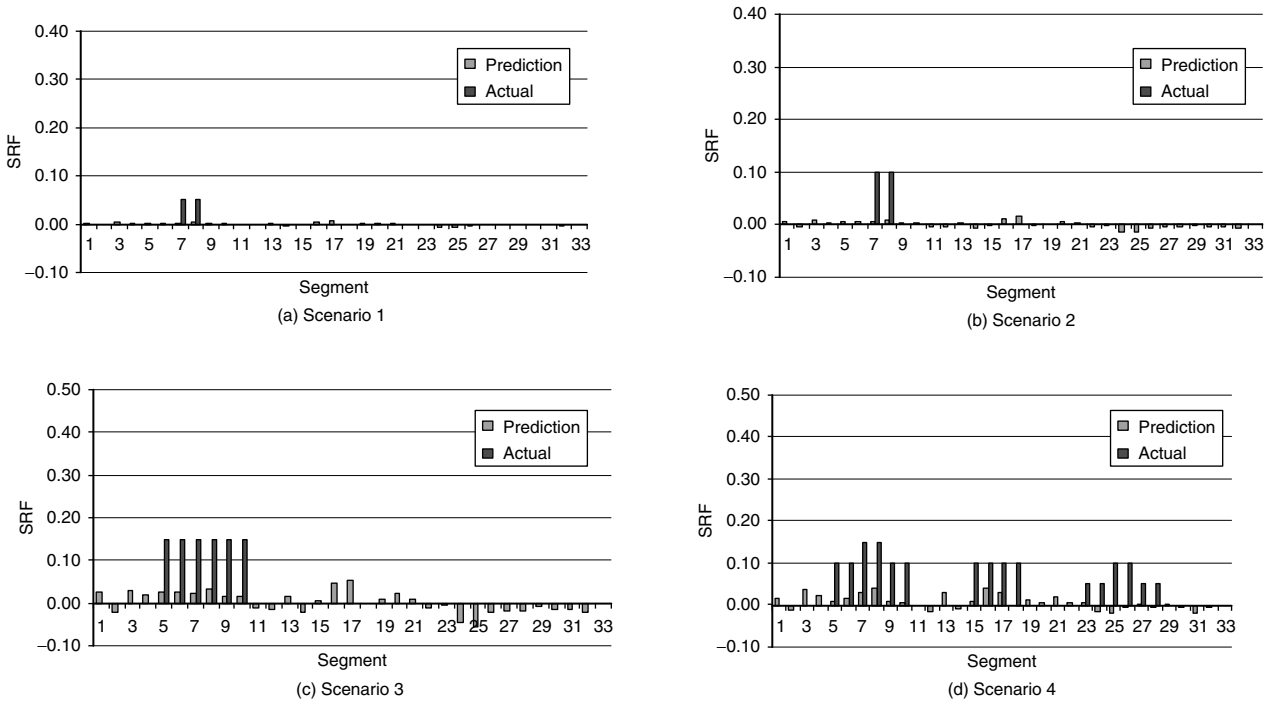

Figure 6. One-stage ANN prediction

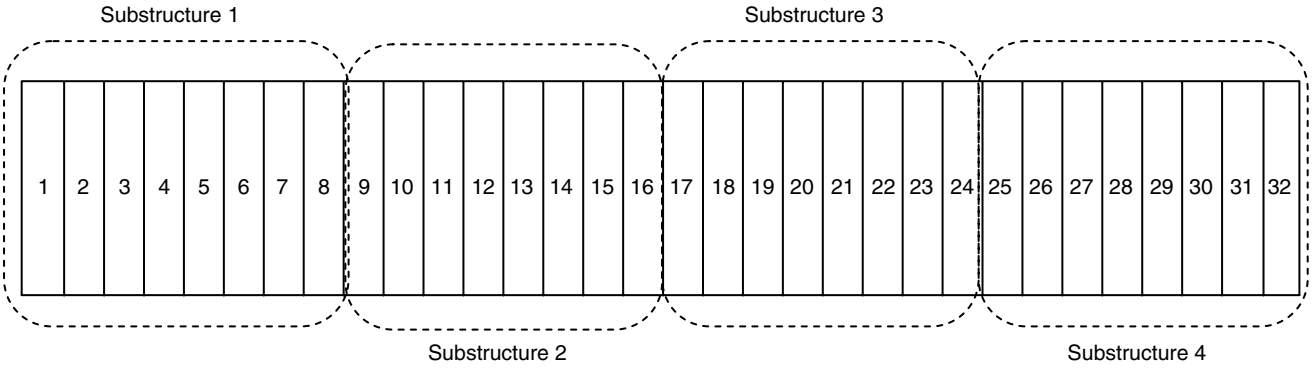

Figure 7. Substructures of the slab

3.2.1. ANN architecture

There are three ANN models in the primary level. NNP1 is used as an intermediate model to generate the frequencies for the ANN models in the second stage. For this purpose the slab is firstly divided into two substructures, each of which is 3.2 m in length. NNP1 is trained to predict the frequencies of these two substructures. The inputs of NNP1 are the first two modal frequencies (f_{full}^1, f_{full}^2) and mode shape values (ϕ_{full}^1, ϕ_{full}^2) of full structure. The outputs of NNP1 are the first three frequencies of the two substructures ($f_{S1sub1}^1 \ldots f_{S1sub1}^3$, $f_{S1sub2}^1 \ldots f_{S1sub2}^3$). The superscripts indicate the number of modes. The subscripts indicate the stage number together with substructure number. At the second stage, the two substructures are further subdivided into four substructures. As shown in the figure, NNP2 and NNP3 are the ANN models at this stage. NNP2 is used to predict the frequencies of substructure 1 and 2 at the second stage ($f_{S2sub1}^1 \ldots f_{S2sub1}^3$, $f_{S2sub2}^1 \ldots f_{S2sub2}^3$), while NNP3 predicts the frequencies of substructure 3 and 4 ($f_{S2sub3}^1 \ldots f_{S2sub3}^3$, $f_{S2sub4}^1 \ldots f_{S2sub4}^3$). The inputs for the ANN models at this stage are the frequencies predicted from the first stage ANN model (NNP1) and the mode shapes of the corresponding substructures. The mode shape values applied to NNP2 and NNP3 are the actual measured mode shape values of the corresponding substructures ($\phi_{S1sub1}^1 \ldots \phi_{S1sub1}^3$, $\phi_{S1sub2}^1 \ldots \phi_{S1sub2}^3$). The outputs of the ANN model in this stage are the three modal frequencies of the four substructures. The conditions of those substructures are examined at this stage. For substructures with identified condition change, the secondary ANN model is built

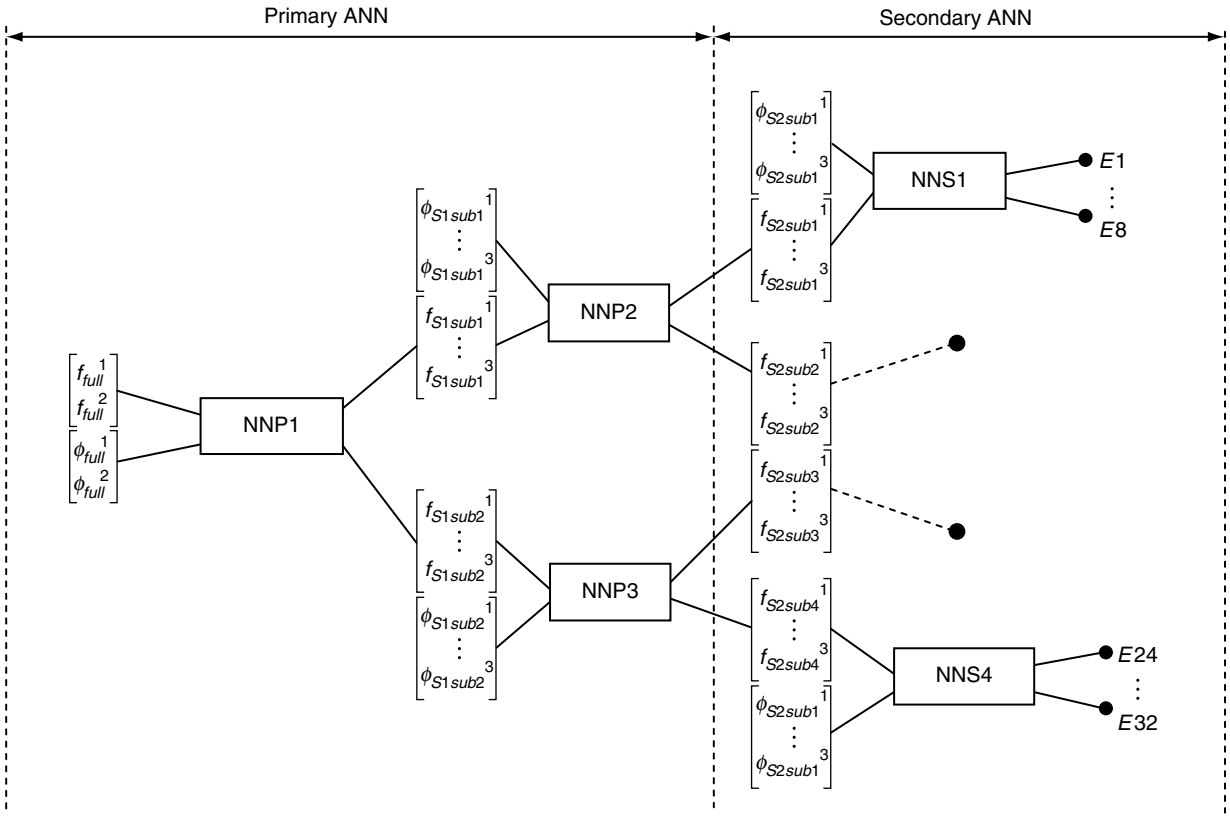

Figure 8. ANN architecture

Table 4. Performance of the primary and secondary ANN models

(a) Performance of the primary ANN

Model	Training performance (MSE)	Validation performance (MSE)	Elapsed time (Second)
NNP1 (62-20-6)	0.0043	0.0057	201.3
NNP2 (48-15-6)	0.0025	0.0028	321.7
NNP3 (48-17-6)	0.0032	0.0048	296.2

(b) Performance of the secondary ANN

Model	Training performance (MSE)	Validation performance (MSE)	Elapsed time (Second)
NNS1 (27-18-8)	0.0652	0.0793	163.3
NNS2 (27-17-8)	0.0787	0.0821	182.1
NNS3 (27-20-8)	0.0773	0.0781	180.3
NNS4 (27-19-8)	0.0814	0.0857	187.2

independently for each of those substructures to predict the location and severity of damage. In this example, the ANN models (NNS1…NNS4) in the secondary level are used to predict the simulated damage scenarios. The outputs are the E values of each segment ($E1 \ldots E32$). The process used in the previous stage is applied again to form the input variables for the corresponding ANN model at this level.

The ANN models are trained individually using the same damage patterns and training algorithm as in the conventional method. The number of hidden nodes is obtained by trial and error. Tables 4(a) and 4(b) lists the performance of ANN models in the primary level and secondary level. It is observed that the MSE values for training and validation are low for all ANN models, indicating that the ANN models are successfully trained

and the relationships between inputs and outputs are established. Moreover, the time required for training the ANN models in primary and secondary level is less than those given in Table 3 for the one-stage ANN model due to the smaller ANN dimension used. Figure 9 shows the calculated FCI values of substructures obtained from the primary ANN. The FCI values indicate condition changes in each substructure, and are used to select the substructures for which it is necessary to build the second level ANN models. Figures 10(a) to 10(d) depict the predicted E values of the slab and the actual simulated damages.

As shown in Figure 9, relatively high FCI values occur only at substructure 1 for damage scenario 1 and 2, while for scenario 3 the high FCI values are observed at both substructure 1 and 2. For scenario 4, the high FCI values occur at every substructure. These results indicate that the substructures that contain damage are correctly identified in the first level. The comparisons between the actual and predicted E values of every segment of the slab are illustrated in Figure 10. As shown, all the damage locations are successfully identified. However, all the SRF values are slightly underestimated. There are also some minor negative false identification in damage scenario 3 and 4, indicting slight stiffness increase in some elements. This is attributed to numerical errors associated with

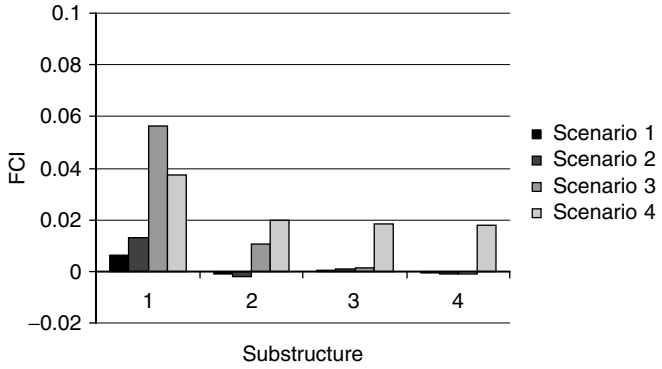

Figure 9. Output of primary ANN

nonlinearity caused by relatively large damage levels in these two scenarios. In comparison with the conventional technique, the proposed approach provides reliable result in terms of damage location and severities. Moreover, by comparing the time required for training the ANN model and predicting the damage with the conventional one-stage ANN model, as given in Tables 3 and 4, the dimensions of the ANN models involved in both stages are smaller and the computational times are also less.

With increasing structural degrees of freedom, using the conventional ANN approach normally requires a large dimension ANN. As shown in the example, to

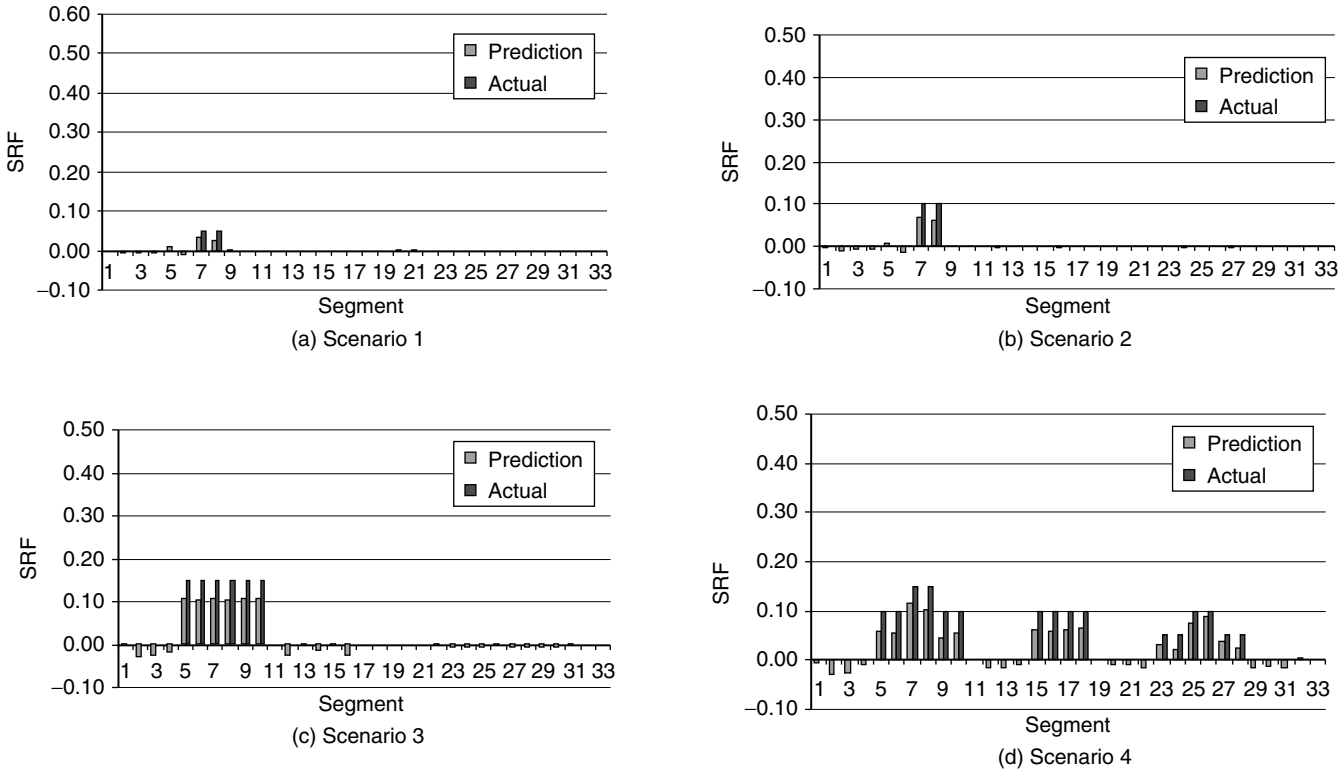

Figure 10. Output of secondary ANN

identify damages in the example analysed in this study using a one-stage ANN model, 32 output nodes are required in the output layer. Thus to develop a well trained ANN, a large size of neurons in the hidden layer is required. Increasing the number of hidden neurons exponentially increases the number of weights in the interconnected neurons of the ANN model. As a result, it requires more computational time and computer memory. For a complex structure with a large number of degrees of freedom, the enormous computer memory requirement and computational cost are prohibitive. Therefore it is not possible to use a single stage ANN for structural damage identification of a real civil structure. Using the proposed substructure method, the size of every ANN model in each stage can be kept small to reduce the computational time and computer memory requirements.

4. SENSITIVITY STUDY

More detailed studies are carried out in this section to investigate the sensitivity of the proposed method with different substructure sizes to damage levels. At this stage, only the primary ANN is involved. The purpose of this study is to determine the level of frequency change index (FCI) of substructures above which a secondary ANN model needs be built for further analyses. Below this level of FCI the substructure is considered not damaged, and no subsequent analysis is needed.

First, an analysis is done to define whether the detectability depends on absolute value of substructure length or the ratio of the substructure length to the span length of the structure. For this purpose, two simply supported concrete girder models with span length 4.8 m and 8 m are analyzed. 400 mm elements are used to model the structure and the modal parameters are obtained using finite element analysis. The material properties are: $E = 2.8 \times 10^{10}\ N/mm^2$, $\rho = 2.45 \times 10^3\ kg/m^3$, $v = 0.2$. Figures 11 (a) and 11(b) shows the finite element model of the structures.

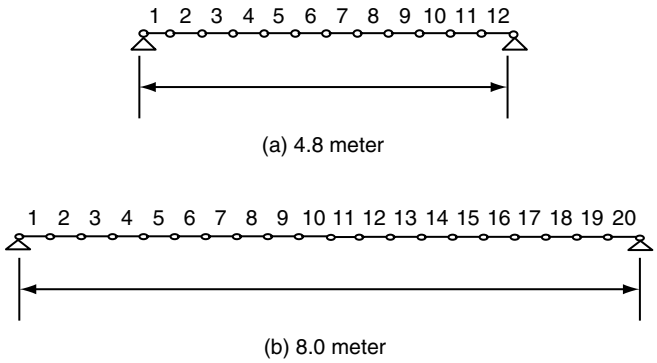

Figure 11. Finite element model of the beams

The structure is divided into two substructures, i.e. the ratio of the substructure length to the span length is 0.5. Three damage levels are introduced to element 5 and 6 in substructure 1. The damage levels are −15%, −10% and –5% in terms of SRF. The outputs of primary ANN for both cases are shown in Figures 12(a) and 12(b).

The output of primary ANN for both cases shows that the FCI values are higher at substructure 1 than substructure 2, indicating the damaged substructure 1 for all levels is correctly identified. However, the FCI values of the 8 m girder is about 30% less than the 4.8 meter girder, and some minor FCI values in substructure 2 are also obtained in the 8 m girder when the damage is 15%, due to numerical errors as discussed above. This indicates the detectability depends on the absolute length of the substructure, instead of the length ratio. When the damage is the same, increase the substructure length will dilute the damage effect on the substructure, thus reduce the FCI values. The results also indicate that a FCI value of 0.05 implies a possible damage of 5% in a length of 0.8 m (two 400 mm elements) in a substructure of length 4 m, whereas the FCI value becomes 0.075 when the substructure is 2.4 m long.

In order to investigate the sensitivity of substructure size to damage level, an analysis is performed by

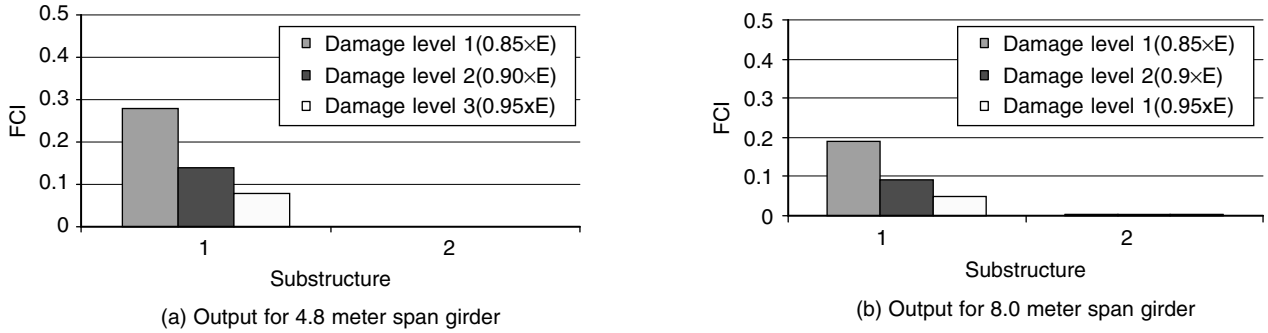

Figure 12. Primary ANN output for 4.8 m and 8.0 m girder

varying the substructure size and damage severity. The same girder as above with a 16 meter span is used in the analysis. Three different substructure sizes are considered, (i) 8 meter, (ii) 4 meter, and (iii) 2 meter. Damage is introduced to element 8 (length 0.4 m) with SRF ranging from –5% to –50% at 0.5% intervals. Figures 13(a) to 13(c) shows the finite element model together with the element number and substructure size. When the substructure is 8 m or 4 m long, the simulated damage is in the first substructure. When it is 2 m long, the damage is in the second substructure. Figures 14 (a) to 14(c) show the output of the primary ANN.

As indicated, the FCI values increase with damage level and reduce with increase of the substructure size. When the substructure is 2 m long, there is no false identification even when the SRF is 5%. When substructure is 4 m or 8 m long, however, some false identification occurs in the undamaged substructure. But

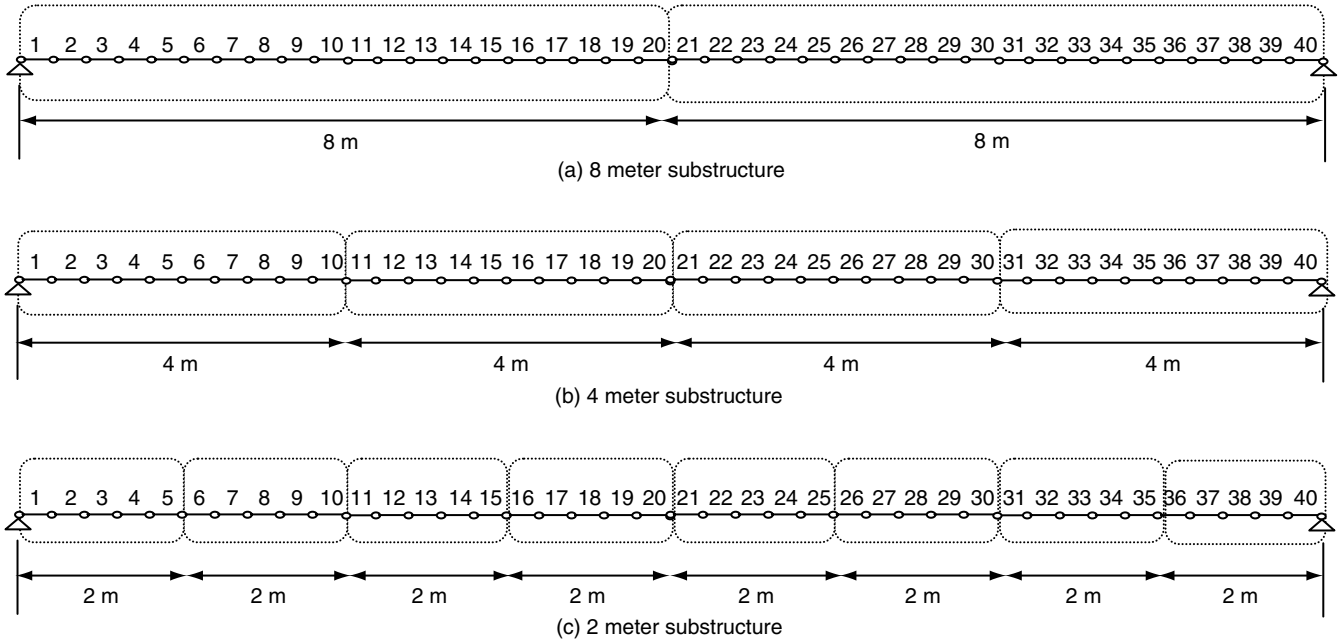

Figure 13. Segmentation of the girder

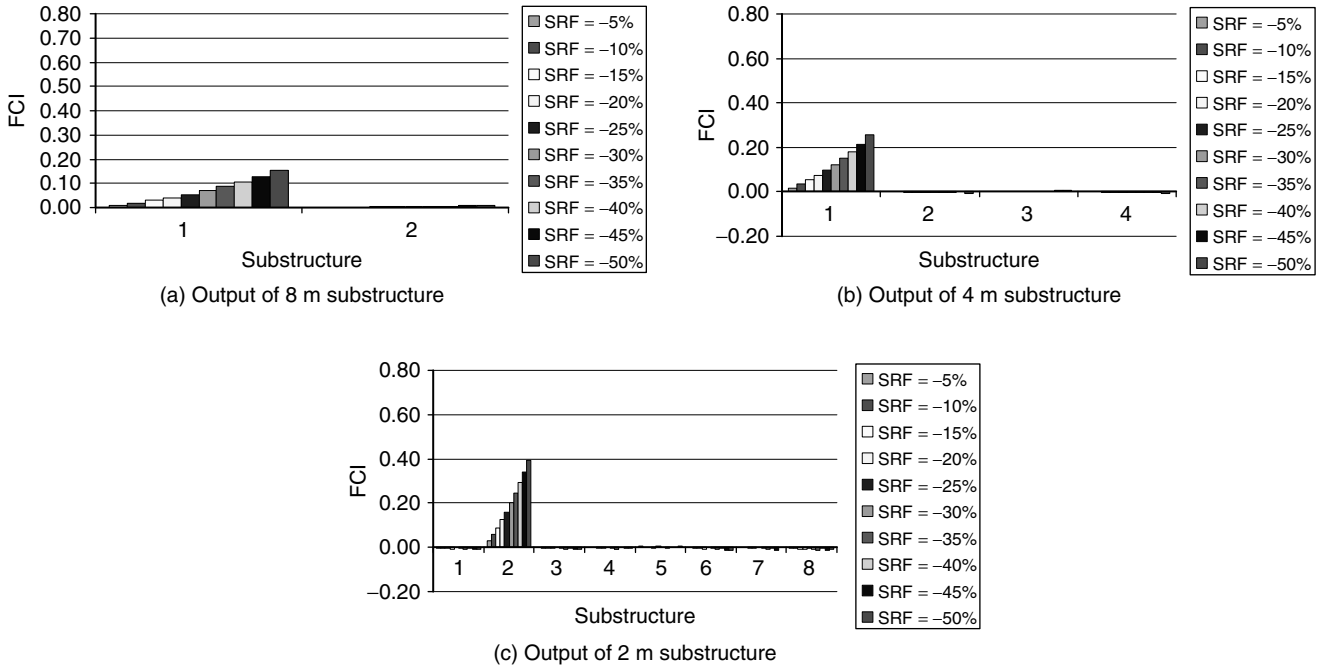

Figure 14. Primary ANN output for 8 m and 4 m and 2 m

this false FCI value is always smaller than the true FCI values when damage is 10% and above.

The effect of boundary conditions and structure type on the relationship between substructure size and damage detectability is also investigated. The three cases considered are: (i) flexible support, (ii) continuous support, and (iii) slab structure. For the flexible support case the pin supports in the previous example are replaced with three parallel spring elements of Young's Modulus $1.9 \times 10^9 N/mm^2$ to simulate the bearing stiffness for bridge structures. For continuous support, an extra pin support is placed at the middle of the girder span. The same damage levels as in the previous analysis are used and the same damage detection process is applied. The numerical results indicate that the relation between the substructure size and the detectable damage level is independent of the structure type and the structure indeterminacy because the results from the continuous beam and slab are similar to those obtained above. However, the flexible boundary conditions affect the relationship between the substructure size and the detectable damage level.

Figure 15 summarizes the numerical results obtained. The solid line is the relationship for the simply supported, continuous and slab structure, while the dashed line is for flexible support case. The area below and above those lines represent detectable and undetectable damage level respectively and the corresponding substructure size. The reason that a smaller substructure is needed to detect same level of damage in the flexible support case is because the spring elements are also damageable. Including spring elements in the substructure increases the number of variables in the analysis, which is equivalent to increase the number of elements in the substructure. If the spring is not considered as a variable in the analysis, the results will then be the same as the case with pin supports.

The above results are based on the assumption that damage occurs in two 400 mm elements only. To study the effect of different damage dimensions with respect to the substructure size, the ratio of the size of damaged elements to the substructure size is varied from 5% to 100%.

Figure 16 illustrates the results. The vertical lines indicate the detectability limit of different ratio between damaged element size (l_{el}) to substructure size (L_{sub}). The area at the right side of the lines represents the detectable damage level. This analysis indicates that if all the elements in a substructure suffer damage, even a small damage can be detected with a large substructure. This is because the ratio l_{el}/L_{sub} significantly affects the vibration frequencies of the substructure.

The above numerical results indicate that damage detectability depends on the substructure size, damage

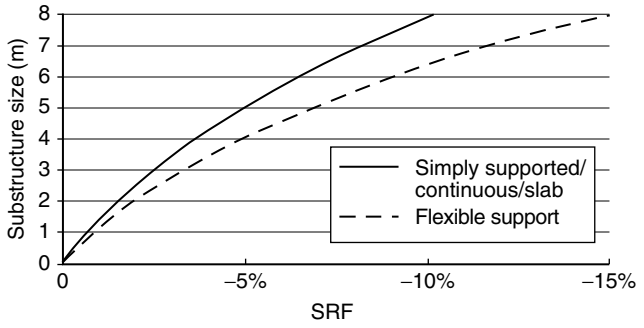

Figure 15. Primary ANN output for different structure conditions

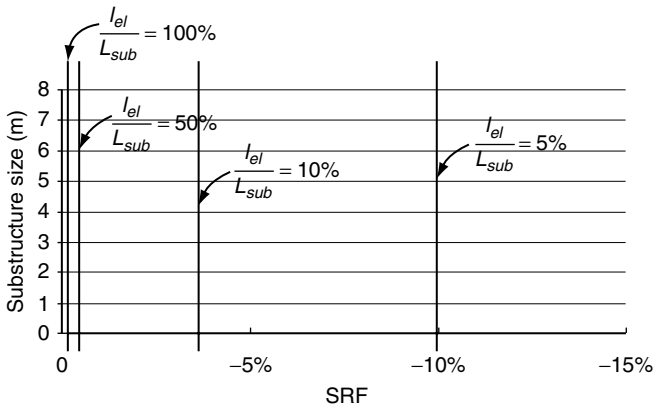

Figure 16. Detectability with respect to the ratios of damaged element size to substructure size

level and the size of the damaged elements in a substructure. It is independent of the structure type and boundary conditions. However, it should be noted that this observation is based on beam-like structures. Further analyses are needed for other structure types such as shell and plate structures.

It should also be noted that the above sensitivity analysis is conducted without considering the modelling errors and measurement noise. In reality, modelling error and vibration measurement noise are inevitable. Various methods have been proposed to take these uncertainties into consideration in structural condition monitoring. For example, Xia and Hao (2003) developed an approximate method based on the Taylor expansion and perturbation to simultaneously model the effects of both the measurement noise and modelling error on structural damage identification. The authors (Bakhary *et al.* 2007) had also modelled simultaneously the measurement noise and modelling error in structural damage identification with ANN approach. It was found that if training and testing data have same uncertainty level, the developed ANN model gives the most reliable structural damage identification. The developed method in the latter study (Bakhary *et al.* 2007) can be

incorporated in the current multi-stage ANN model with substructuring approach in structural damage identification. However, detailed discussion of uncertainty effect is not given here because the primary objective of this paper is to introduce the proposed substructuring technique and to demonstrate its applicability in identifying conditions of large structures, also because of the paper length limitation.

5. NUMERICAL EXAMPLE 2

To further demonstrate the efficiency of the proposed approach, a single span two-storey frame as shown in Figure 17 is considered. The modulus of elasticity is taken as 2.8×10^{10} N/mm^2 and the mass density as 2450 kg/m^3. The cross section of the beams and columns are shown in the figure. Rigid connections between the beams and the columns are assumed, and the supports are assumed to be fixed. The frame is modelled with 24 elements and 23 nodes. Each element is 1500 mm in length. Modal analysis is conducted using finite element analysis. Two damage cases are generated to demonstrate the proposed approach. Case 1 consists of damage at a second floor beam while for Case 2 the damage is at Joint 1 and 2. The damage severities together with the elements and substructures involved for each case are listed in Table 5. The first three frequencies for the undamaged and damaged cases are given in Table 6. To apply the proposed approach, the frame is divided into three substructures. Each substructure representing one floor consists of 8 elements.

For training, damage cases are generated based on orthogonal array 24.12.2.3. For each damage case 42 different severities are generated using Latin hypercube sampling, resulting 1008 training cases. 240 damage cases generated with the same method are used for validation purposes. Only one ANN model is developed for primary ANN. The first three modal frequencies and mode shapes are used as the inputs, and the outputs are the first three modal frequencies of each substructure.

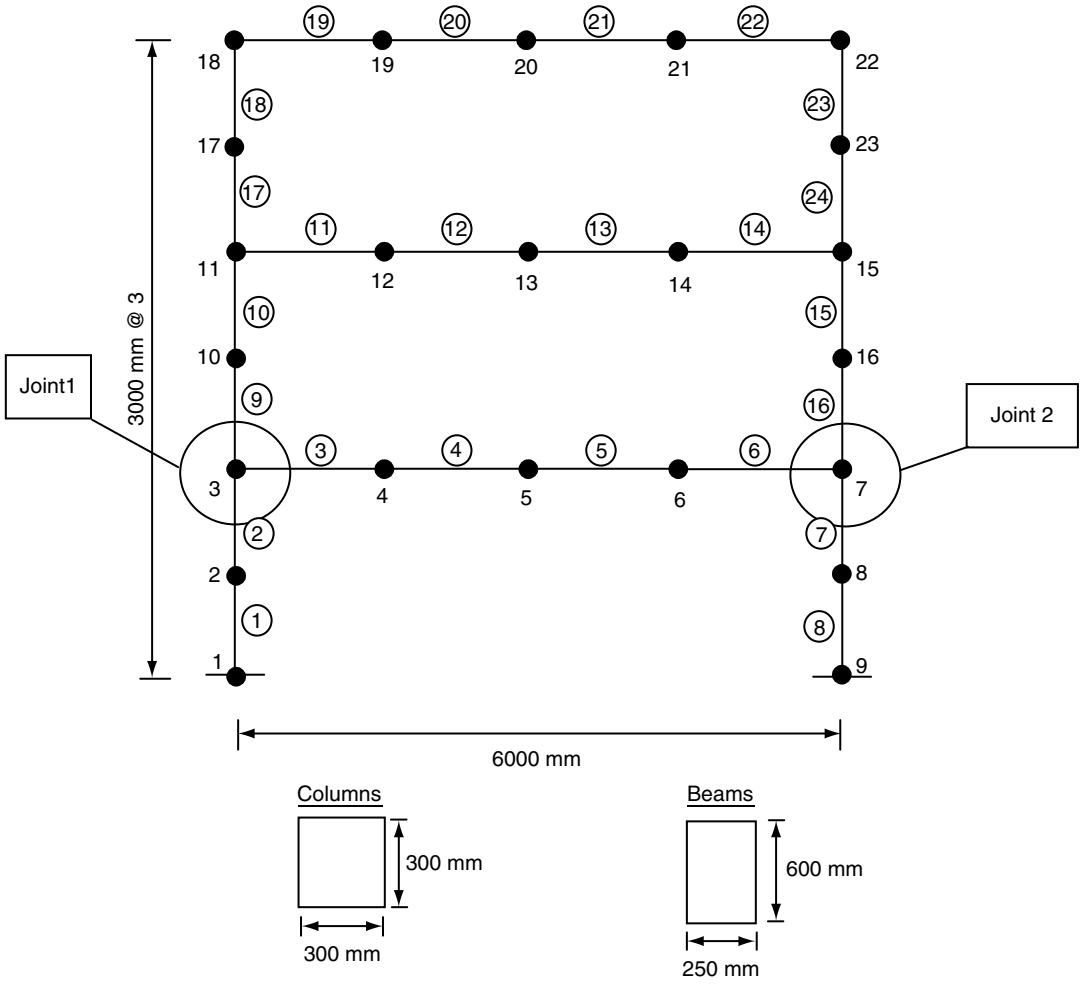

Figure 17. Finite element model of the frame

Table 5. Damage cases for frame

Case	Structure	Element	E value	Substructure
1	Beam	11	0.90 × E	
		12	0.90 × E	2
		13	0.90 × E	
		14	0.90 × E	
2	Joint 1	2	0.85 × E	Joint 1
		3	0.85 × E	Joint 1
		9	0.85 × E	
	Joint 2	6	0.85 × E	
		7	0.85 × E	
		16	0.85 × E	

Table 6. First three frequencies of the frame corresponding to the different damage stage (H_z)

	Undamaged	Case 1	Case 2
Mode 1	4.12	4.09	3.99
Mode 2	13.05	13.00	12.82
Mode 3	20.91	20.78	20.40

The mode shapes used are specified by the x-translations of the columns and the y-translation of the beams. Figures 18(a) and 18(b) show the FCI values predicted from the primary ANN model for case 1 and case 2.

It is observed that for both cases a higher FCI value occurred at the substructure that contains the damage, indicating the damaged substructures for both cases are correctly identified. For case 1, only one secondary ANN model is developed for substructure 2 to determine the damage, whereas for case 2, two secondary ANN models are developed for substructures 1 and 2. By using the method described above, ANN models for corresponding substructures are then trained and tested. Figures 19 (a) and 19(b) shows the identification results. From the figure, it is observed that the damaged elements for both cases are all correctly identified. However, it is also noticed that the damage severities for both cases are underestimated. This may be because the variation of the damage cases used in the training of secondary ANN is large, and thus the testing data is not close enough to the training data. This can be improved if more training data in the secondary stage is generated and used to train the model.

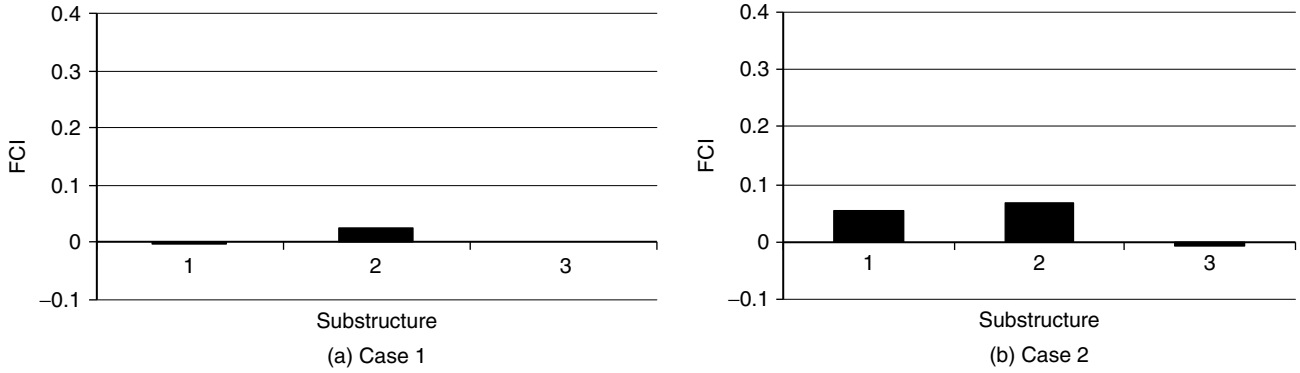

Figure 18. Output of the primary stage

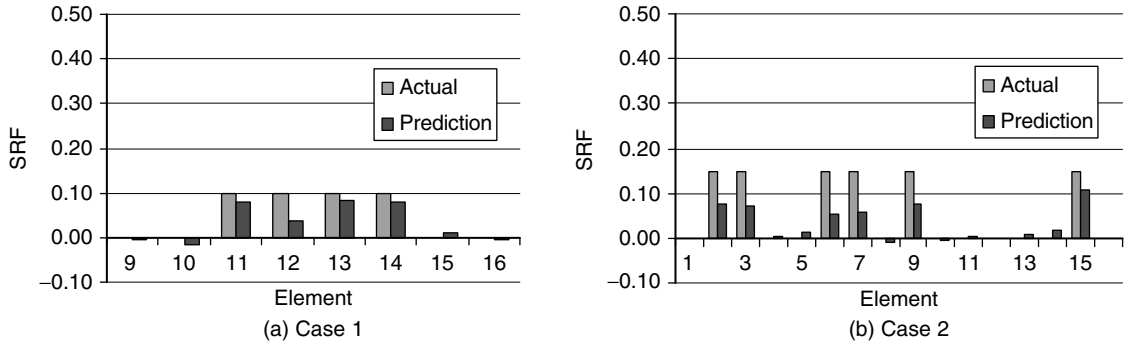

Figure 19. Output of the secondary stage

6. CONCLUSION

This study presented a new approach for applying ANN for damage identification. A substructuring technique is employed together with a multistage ANN to detect local damage in structures. A comparison with the conventional technique demonstrated the efficiency and reliability of the proposed approach. This study also demonstrated that using a one-stage ANN model for damage detection of large structures requires excessive computational time and a large amount of computer memory. The proposed approach is effective in reducing the size of the required ANN models, and as a result the computational effort can be reduced substantially. The results show that by dividing the full structure into substructures and analysing each substructure independently, local damage can be better identified. The proposed approach can also be reliably and efficiently used to identify multiple damages in multiple substructures, thus overcoming the difficulties present in the multiple stage method proposed by Ko *et al.* (2002), which requires expensive computations when multiple damage locations exist in the structure. In comparison with the work by Yun and Bahng (2000), which requires other means such as visual inspection to approximately locate the damage before applying ANN, the proposed approach identifies damages in structures directly from the modal parameters of the structure.

ACKNOWLEDGEMENT

Financial support from the Universiti Teknologi Malaysia for the first author to pursue a PhD study at University of Western Australia is gratefully acknowledged. The authors also acknowledge the partial financial support from Australian Research Council (ARC) under grant number DP0881582.

REFERENCES

Bakhary, N., Hao, H. and Deeks A. (2007). "Damage detection using artificial neural network with consideration of uncertainties", *Engineering Structures*, Vol. 29, No. 11, pp. 2806–2815.

Barai, S.V. and Pandey, A.K. (1995). "Vibration signature analysis using artificial neural network", *Journal of Computing in Civil Engineering*, Vol. 9, No. 4, pp. 259–265.

Cawley, P. and Adams, R.D. (1979). "The location of defects in structures from measurements of natural frequencies", *Journal of Strain Analysis*, Vol. 14, No. 2, pp. 49–57.

Chang, C.C., Chang, T.Y.P. and Xu, Y.G. (2000). "Structural damage detection using an iterative neural network", *Journal of Intelligence Material Systems and Structure*, Vol. 11, No. 1, pp. 32–42.

Chen, Y.M. and Lee, M.L.. (2002). "Neural networks-based scheme for system failure detection and diagnosis", *Mathematics and Computers in Simulation*, Vol. 58, No. 2, pp. 101–109.

Hurty, W.C. (1964). "Dynamic analysis of structural systems using component modes", *AIAA Journal*, Vol. 3, No. 4, pp. 678–684.

Ko, J.M., Sun, Z.G. and Ni, Y.Q. (2002). "Multi-stage identification scheme for detecting damage in cable-stayed Kap Shui Mun bridge", *Engineering Structures*, Vol. 24, No. 7, pp. 857–868.

Koh, C.G., Hong, B. and Liaw, C.Y. (2003). "Substructural and progressive structural identification method", *Engineering Structures*, Vol. 25, No. 12, pp. 1551–1563.

Lee, J.W., Kim, J.D., Yun, C.B., Yi, J.H. and Shim, J.M. (2002). "Health-monitoring method for bridges under ordinary traffic loadings", *Journal of Sound and Vibration*, Vol. 257, No. 2, pp. 247–264.

Ni, Y.Q., Zhou, X.T., Ko, J.M. and Wang, B.S. (2000). "Vibration-based damage localization in Ting Kau Bridge using probabilistic neural network", in *Advances in Structural Dynamics*, Hong Kong.

Oreta, W.C. and Tanabe, T. (1994). "Element identification of member properties of framed structures", *Journal of Structural Engineering*, ASCE, Vol. 120, No. 7, pp. 1961–1976.

Pillai, P. and Shankar, K. (2008). "A hybrid neural network strategy for identification of structural parameters", *Journal of Structure and Infrastructure Engineering*, Vol. 15, No. 1, pp. 1–13.

Worden, K. (1997). "Structural fault detection using novelty measure", *Journal of Sound and Vibration*, Vol. 201, No. 1, pp. 85–101.

Wu, X., Ghaboussi, J. and Garrett, J.H. (1992). "Use of neural networks in detection of structural damage", *Computers & Structures*, Vol. 42, No. 4, pp. 649–659.

Xu, H. and Humar, J. (2006). "Damage detection in a girder bridge by artificial neural network technique", *Computer-Aided and Infrastructure Engineering*, Vol. 21, No. 6, pp. 450–464.

Yuen, K.V. and Katafygiotis, L.S. (2006). "Substructure identification and health monitoring using noisy response measurement only", *Computer-Aided and Infrastructure Engineering*, Vol. 21, No. 4, pp. 280–291.

Yun, C.B. and Bahng, E.Y. (2000). "Substructural identification using neural networks", *Computers & Structures*, Vol. 77, No. 1, pp. 41–52.

Xia, Y. and Hao, H. (2003). "Statistical damage identification of structures with frequency changes", *Journal of Sound and Vibration*, Vol. 263, No. 4, pp. 853–870.

Zapico, J.L., Gonzalez, M.P. and Worden, K. (2003). "Damage assessment using neural network", *Mechanical Systems and Signal Processing*, Vol. 17, No. 1, pp. 119–125.

Zhao, J., Ivan, J.N. and DeWolf, J.T. (1998). "Structural damage detection using artificial neural network", *Journal of Infrastructure Systems*, ASCE, Vol. 4, No. 3, pp. 93–101.